Dry reforming of methane on porous membrane catalytic systems*

M. V. Tsodikov,[a] V. V. Teplyakov,[a] A. S. Fedotov,[a] N. Yu. Kozitsyna,[b] V. Yu. Bychkov,[c] V. N. Korchak,[c] and I. I. Moiseev[a]*

[a]*A. V. Topchiev Institute of Petrochemical Synthesis, Russian Academy of Sciences, 29 Leninsky prosp., 119991 Moscow, Russian Federation. Fax: +7 (495) 633 8520. E-mail: tsodikov@ips.ac.ru*
[b]*N. S. Kurnakov Institute of General and Inorganic Chemistry, Russian Academy of Sciences, 31 Leninsky prosp., 119991 Moscow, Russian Federation. Fax: +7 (495) 954 1279*
[c]*N. N. Semenov Institute of Chemical Physics, Russian Academy of Sciences, 4 ul. Kosygina, 119991 Moscow, Russian Federation. Fax: +7 (495) 651 2191*

A method of high-performance dry reforming of methane into syngas at temperatures below 650 °C on membrane catalytic systems was proposed. The membrane catalytic systems consist of porous inorganic membrane-supports, prepared by self-propagating high-temperature synthesis and modified by nanosized metallocomplex components, which are uniformly distributed inside membrane pores. The influence of the composition of the supported active components, temperature, and flow rate on the activity and selectivity of CH_4 and CO_2 transformations into syngas, as well as the dynamics of CH_4 and CO_2 conversion on the membrane catalytic systems were studied.

Key words: membrane catalytic systems, porous inorganic membranes, microreactor, syngas, dry methane reforming.

Production of valuable products from non-petroleum raw materials is among the most important problems of modern industry of heavy organic synthesis. Special attention is given to efficient processes of reforming of natural gas and other C_1-substrates of synthetic and technogenic origin, including substrates obtained from renewable biomass.[1] The development of the process of combined methane and carbon dioxide reforming is of practical interest for the rational use of carbon from industrial flue gases and biogas. High thermodynamic stability of CH_4 and CO_2 molecules impedes this problem. Nevertheless, both these components of biogas belong to promising non-petroleum resources for the production of important carbon-containing products and hydrogen.

Considerable developments can be expected from the reforming of methane and carbon dioxide in the reactor unit of membrane catalytic systems (MCS). Membrane systems are traditionally used in catalytic processes to diminish energy expenses at the step of preparation of raw materials for further catalytic treatment or in selective separation of reaction products.[2] However, increased attention is recently given to gas-phase heterogeneous catalytic reactions of C_1-substrates in microreactors. Catalytic setups based on microreactors have small sizes, which simplifies a designing task and thus makes it possible to replicate rather than scale up the membrane reactor unit.[3,4] Channels of porous membranes modified by highly dispersed nanosized catalytic systems can serve as microreactors. The number of channels with an effective cross-section of 3 μm is up to 10^7 per square centimeter of the membrane. The catalyst formed inside the membrane channels is characterized by a high active surface and a small volume of transport pores.

The purpose of this work is to study the process of dry reforming of methane (DRM) on the MCS.

Experimental

Unique tubular ceramic membranes produced by self-propagating high-temperature synthesis (SHTS)[5,6] were used.

Bimetallic catalytic systems based on organic solutions of metallocomplex precursors Pd—Co, Pd—Zn, Pd—Mn,[7] and Re—W (see Ref. 8) and La^{III} and Ce^{IV} nitrates[9] in the internal volume of the membrane channels were formed by the alkoxo method.[6]

According to the published data[9] describing DRM in a traditional fixed-bed reactor, the catalytic system based on La—Ce has the highest activity. The catalytic systems containing the

* Dedicated to Academician S. N. Khadzhiev on the occasion of his 70th birthday.

Published in Russian in *Izvestiya Akademii Nauk. Seriya Khimicheskaya,* No. 1, pp. 54—61, January, 2011.

1066-5285/11/6001-55 © 2011 Springer Science+Business Media, Inc.

active components Pd—M (M = Co, Zn, Mn) and Re—W were also used.[7,8]

Prior to introducing catalytically active species, a buffer layer of TiO_2 was incorporated onto the internal walls of the membrane channels. This allows an increase in the specific surface and a decrease in the pore size. A colloidal mother liquor of titanium *n*-butylate stabilized by acetylacetone was pumped through microchannels of the membrane. The amount of TiO_2 introduced was monitored by an increase in the weight registered when the membrane was coated with TiO_2 and then thermally treated. The procedure of loading was repeated 4—6 times until the content of the layer supported on the membrane reached 3.2—3.5 wt.% TiO_2. After the buffer layer of TiO_2 was incorporated, the metallooxide catalytic coating was formed.[10]

Catalytic coatings on the inner surface of the membrane channels were formed by pumping organic solutions of catalytic precursors through the membrane on the laboratory setup (Fig. 1). Then wet heated air was blown through the membrane, and the membrane was dried *in vacuo* (1 Torr) and heated in various temperature regimes to remove organic moieties. Thermal treatment of the bimetallic catalytic systems Pd—M and Re—W can be accompanied by the destruction of organic bridges between metals, where by metal atoms are brought together to form new heterometallic compounds.

The lanthanum—cerium catalyst ([La—Ce]—MgO—TiO_2/Ni—Al) was formed by successive introduction of magnesium acetylacetonate stabilized by monoethanolamine in a toluene solution. After thermal treatment of the magnesium-containing coating, a mother liquor of the lanthanum and cerium chelated complexes in methanol were introduced on the inner surface of the membrane. Then the membrane was treated in an exhaust box in a flow of wet heated air, evacuated for 45 min at 80 °C, and subjected to thermal treatment in a muffle furnace at 500 (30 min), 600 (30 min), and 700 °C (4 h) to remove organic moieties.

Titanium *n*-butylate was used along with heterometallic acetate complexes Pd(μ-OOCMe)$_4$Co(OH$_2$) (**1**), Pd(μ-OOCMe)$_4$Zn(OH$_2$) (**2**), and Pd(μ-OOCMe)$_4$Mn(OH$_2$) (**3**) to form the Pd—M-containing catalytic systems in the internal volume of the ceramic membrane.

A colloidal solution containing complexes **1—3** was prepared as follows: titanium *n*-butylate was diluted with anhydrous toluene in a volume ratio of 1 : 1 in an argon flow, and acetylacetone was added in the molar ratio M : Ti(OC$_4$H$_9$)$_4$: AcAcH = 1 : 1 : 1. The resultant system was magnetically stirred for 30 min at 20 °C.

Acetate complexes **1—3** in an amount necessary for the preparation of the oxide systems Pd—M/TiO_2 with the content of 2% Pd and 1% M with respect to the buffer layer of TiO_2 were dissolved in methanol at 20 °C. The obtained 2% solutions of the bimetallic Pd-containing acetate complexes were added with stirring in an Ar flow to the stabilized solution of titanium butylate. The resultant mixture was magnetically stirred for 30 min in an Ar flow.

Complex $Re_{4-x}W_xO_{6-y}(OCH_3)_{12+y}$ synthesized by the electrochemical method[8] and titanium tetrabutylate were used for the formation of the Re—W coating as initial reagents for the preparation of the sol containing rhenium and tungsten. A methanolic solution of the Re—W complex in an amount necessary for the introduction of 5 wt.% rhenium and tungsten into titania was added under Ar atmosphere to the stabilized solution of titanium tetrabutylate, and the mixture was stirred for 30 min.

Sol was introduced on the modified membrane according to the procedure described above. After each layer was incorporated, the membrane was dried in a desiccator at 60 °C, organic moieties were removed by thermal impact at 500 °C in a muffle furnace under an Ar flow. The procedure was repeated 4 times. The final thermolysis for the formation of catalytic metallooxide was carried out at 500 °C in an Ar flow for 5 h.

The content of active components in the MCS channels is given in Table 1.

The schemes of the laboratory membrane catalytic test bench and reactor are presented in Figs 2 and 3, respectively.

The process of DRM was conducted at 350—800 °C and a pressure at the inlet of the reactor lower than 5 atm with a pressure at the outlet 1 atm, and a flow rate of the initial gas mixture ($CH_4/CO_2 = 1$) lower than 400 L h^{-1}. Pure gaseous methane (99.9 vol.%, TU 51-841-87) and gaseous high-purity carbon dioxide (99.995 vol.%, GOST 8050-85) were used. Since the mechanical resistance of the membrane to compression is higher than to tension, gaseous substrates were fed to the external side of the membrane.

The compositions of the substrate and reaction products were determined by gas chromatography on a Chrom-5 chromatograph using a katharometer as a detector and high-purity argon

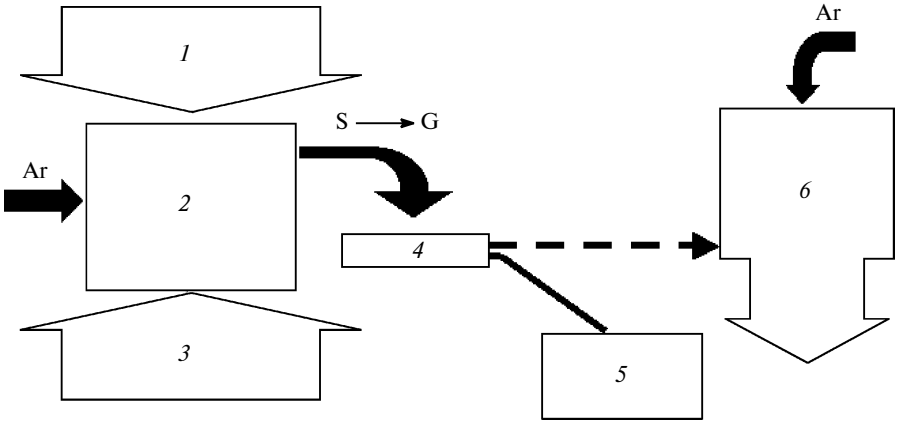

Fig. 1. Modification of the inner surface of channels of the membranes with the catalytic coating: *1*, precursors; *2*, organic colloidal solution; *3*, solvent, sol stabilizers; *4*, membrane; *5*; vacuum pump; *6*, muffle furnace; S is mother liquor, and G is gel.

Table 1. Content of the active components on the MCS

Active component		Content (wt.%)*	
I	II	I	II
La	Ce	0.0200	0.0350
Pd	Mn	0.0150	0.0080
Pd	Co	0.0140	0.0070
Pd	Zn	0.0300	0.0150
Re	W	0.0530	0.0530

* Based on the weight of the membrane (~100 g).

(content of argon at least 99.998 vol.%, TU 6-21-12-94, flow rate 30 mL min^{-1}) as a carrier gas, and a packed chromatographic column 1 m×3 mm filled with active carbon (SKT trade mark, 0.2—0.3 mm). The concentrations of CO and CO_2 were determined by IR spectroscopy using Riken Keiki RI-550A sensors.

The dynamics of macrokinetic steps of DRM on the MCS and the process as a whole was studied on a precision setup including a gravimetric cell (Fig. 4), a high-precision thermobalance, and a mass spectrometer.

The change in the weight of the samples during experiment was detected using a SETSYS Evolution high-precision thermobalance. Samples in a flow of the mixture $CH_4/CO_2 = 1$ (20 mL min^{-1}) were heated from 30 to 700 °C with a rate of 10 °C min^{-1} and stored for ~2 h at 700 °C. Then the system was evacuated and cooled to 30 °C, after which the sample was heated in a CO_2 flow (20 mL min^{-1}) in the temperature-programmed regime (30—700 °C, 10 °C min^{-1}) and stored for 10 min at 700 °C. The sample was cooled in a CO_2 flow to 30 °C, heated repeatedly under the conditions indicated above in a flow of a CH_4—CO_2 mixture, and stored for 2 h at 700 °C.

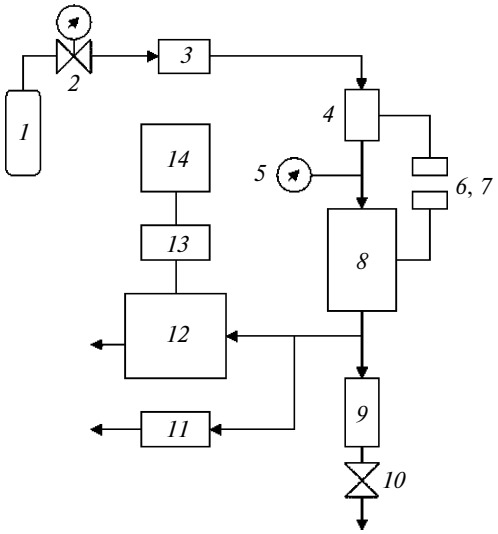

Fig. 2. Scheme of the membrane catalytic test bench: *1*, initial gas mixture; *2*, reductor; *3*, regulator of gas flow; *4*; preheating furnace; *5*, manometer; *6* and *7*, thermocouples; *8*, heated membrane reactor (Fig. 3); *9*, vessel for collection of liquid; *10*, shut-off valve; *11*, CO- and CO_2-analyzers; *12*, chromatograph; *13*, analog-to-digital converter; and *14*, computer.

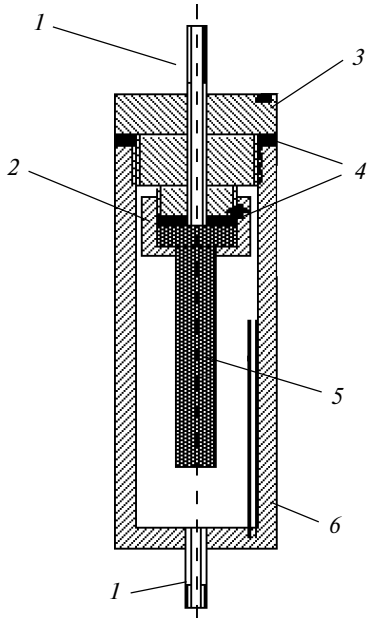

Fig. 3. Membrane reactor: *1*, inlet—outlet nipple; *2*, fastening nut of membrane; *3*, cap of reactor; *4*, cellular-graphite gaskets; *5*, catalytic membrane; and *6*, pocket for thermocouple.

Results and Discussion

The membrane catalytic systems represent porous ceramic supports (membranes) modified by nanosized metallocomplex catalysts. For the initial membranes mechanical strength, catalytic activity, and stability are the most overriding considerations. For this purpose. we

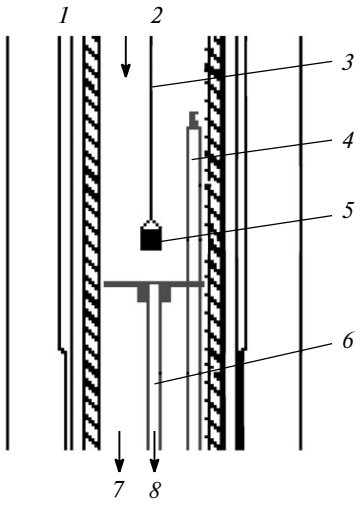

Fig. 4. Thermogravimetric cell: *1*, furnace; *2*, initial gas mixture at inlet of reactor; *3*, quartz filament; *4*; thermocouple; *5*, suspended cell with sample; *6*, aluminum capillary for sampling gas mixture behind sample to analysis in mass spectrometer; *7*, product gas mixture at outlet of reactor; and *8*, gas flow to mass spectrometer.

Table 2. Parameters of DRM on various MCS*

Support	Catalyst	Productivity, ρ_{membr}/L h^{-1} dm^{-3}	H_2/CO	Conversion (vol.%)	
				CH_4	CO_2
Ni—Al—FeC	—	176	0.07	9.0	3.3
Ni—Al (pelleted)	La—Ce	249	0.66	10.3	6.8
Ni—Al	—	327	0.10	13.5	1.4
	Pd—Co	708	0.20	25.3	9.9
	Re—W	1084	0.68	23.1	19.0
	Pd—Zn	1790	0.96	34.3	34.3
	Pd—Mn	3344	1.25	46.8	31.5
	La—Ce	3780	0.63	51.2	26.1
Ni—Al—Co	—	344	0.36	13.9	6.2
	La—Ce	516	0.42	20.9	9.3
Ni—Ti	—	2171	0.55	43.3	29.8

* Conditions: $T = 600$ °C, $W_{inlet} = 40$ L h^{-1}, $CH_4/CO_2 = 1$.

synthesized four types of membranes in the form of tubular structures: Ni—Al—FeC, Ni—Al, Ni—Al—Co, and Ni—Ti. The catalytic activity of the membranes is listed in Tables 2 and 3.

The productivity for syngas was taken as a measure of catalytic activity of the sample during DRM.

It turned out that the membrane containing cementite (Ni—Al—FeC) possessed the highest strength; however, the catalytic activity of this membrane is very low.

The membrane Ni—Al—Co proved to be the second in strength, but its modification by the metallooxide catalysts does not substantially increase the catalytic activity (see Table 2, example La—Ce/Ni—Al—Co).

The membrane Ni—Ti is rather active in DRM but does not meet requirements of mechanical strength. The most probable reason is the active absorption of hydrogen by titanium at 600 °C to form brittle hydrides, which results in the fast decomposition of the sample.

The Ni—Al membrane possesses optimal properties and, therefore, it was selected for the formation of the membrane catalytic systems.

The data in Table 2 show rates of the DRM on the MCS with the content of the catalytic components varying from 0.021 to 0.055 wt.% (see Table 1) supported on the internal surface of the membrane channels. The rates exceed the rate of this process on the non-modified membrane and in a traditional fixed-bed reactor with the catalyst of the same composition, taken in the same amount, and obtained by membrane grinding by more than an order of magnitude. The composition of the syngas formed changes noticeably with a change in the composition of the supported active components.

Compared to the monometallic catalysts containing La and Ce as active components, the non-additive increase in the catalytic activity has earlier[11] been found for DRM in the traditional reactor on the catalyst La—Ce/MgO. In this case, appreciable transformations of methane and carbon dioxide are observed at temperatures above 750 °C,[10] whereas on the MCS considerable conversions are observed at much lower temperatures (Fig. 5).

It is found that on the MCS [La—Ce]—MgO—TiO_2/Ni—Al (**4**) the initiation temperature of the process is

Table 3. Activity of the MCS in the DRM process (TOF)*

MCS	TOF $(CH_4 + CO_2)/h^{-1}$
La—Ce/Ni—Al	1030
Pd—Mn/Ni—Al	834
Pd—Co/Ni—Al	790
Pd—Zn/Ni—Al	343
Re—W/Ni—Al	289

* Conditions: $CH_4/CO_2 = 1$, $T = 600$ °C, $W_{inlet} = 40$ L h^{-1}. TOF is turnover frequency (measure of activity of the catalyst based on 1 g-atom of the active component).

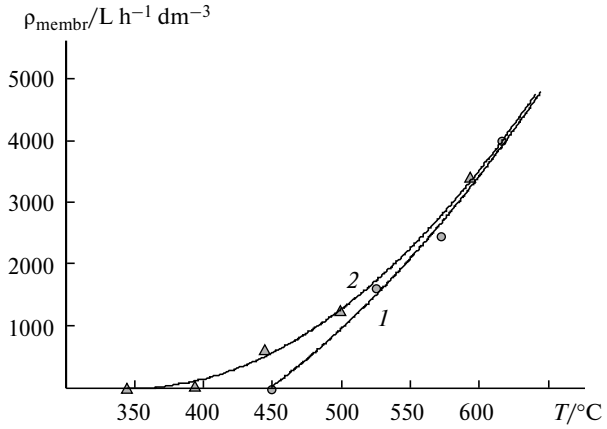

Fig. 5. Temperature plots of the productivity for syngas on the MCS [La—Ce]—MgO—TiO_2/Ni—Al (*1*) and [Pd—Mn]-TiO_2/Ni—Al (*2*).

more than 50 °C higher than that on [Pd—Mn]—TiO_2/Ni—Al (**5**) (see Fig. 5).

As can be seen from Fig. 6, the maximum productivity of the both systems at 600—650 °C and a residence contact time of 0.1 s can reach 10 500 L h^{-1} dm^{-3}_{membr}, and the H_2/CO ratio on the MCS [Pd—Mn]—TiO_2/Ni—Al (**5**) is higher than on lanthanum—cerium system **4** (see Table 2).

The difference in compositions of syngas formed on MCS **4** and **5** is due to different rates of methane and carbon dioxide conversion on these catalysts. As follows from Figs 7 and 8, with an increase in the temperature of the process, the rates of CO_2 and methane transformation are closer on the system Pd—Mn (**5**) than those on the La—Ce-containing system (**4**).

Dynamics of methane and carbon dioxide transformation on the MCS. As follows from the gravimetric data (Fig. 9), a noticeable weight loss of the sample of the initial membrane Ni—Al is observed when the sample is heated to ~550 °C.

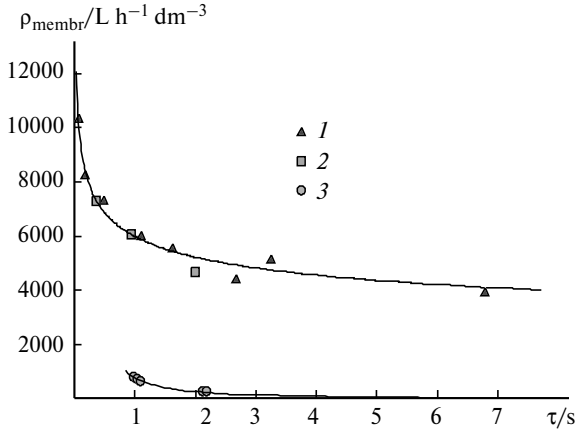

Fig. 6. Productivity for syngas *vs* duration on contact for the MCS [La—Ce]—MgO—TiO_2/Ni—Al (*1*) and [Pd—Mn]—TiO_2/Ni—Al (*2*), and the initial Ni—Al membrane (*3*).

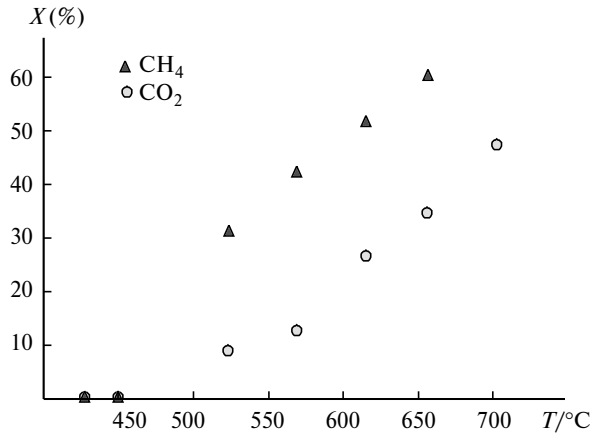

Fig. 7. Temperature dependence of the conversion of CH_4 and CO_2 on the MCS [La—Ce]—MgO—TiO_2/Ni—Al ($CH_4/CO_2 = 1$, $W_{inlet} = 40$ L h^{-1}).

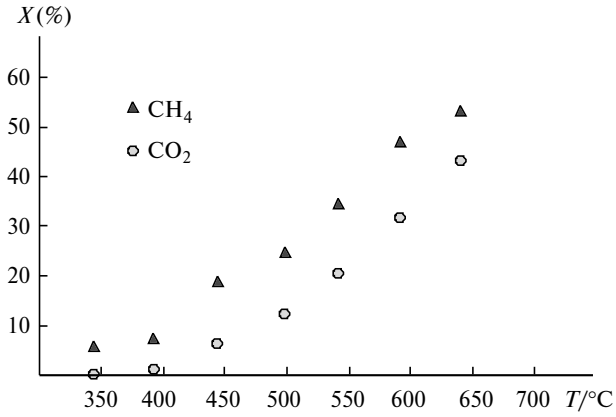

Fig. 8. Temperature dependence of the conversion of CH_4 and CO_2 on the MCS [Pd—Mn]—TiO_2/Ni—Al ($CH_4/CO_2 = 1$, $W_{inlet} = 40$ L h^{-1}).

The mass spectrometric data show that the decrease in the weight is accompanied by the formation of H_2, CO, CO_2, and H_2O (Fig. 10).

It cannot be excluded that the sample weight decreases during oxidation of methane with surface oxygen O_s of the oxide phases of metals of the membrane material that are formed at the step of preparation of the membrane

$$CH_4 + O_s \longrightarrow CO + 2\,H_2, \quad (1)$$

$$CH_4 + 4\,O_s \longrightarrow CO_2 + 2\,H_2O. \quad (2)$$

It is seen from Fig. 10 that on gradual heating the sample weight begins to increase again until the temperature maximum of the experiment (700 °C) is achieved. It is most probably that the weight increase is due to the

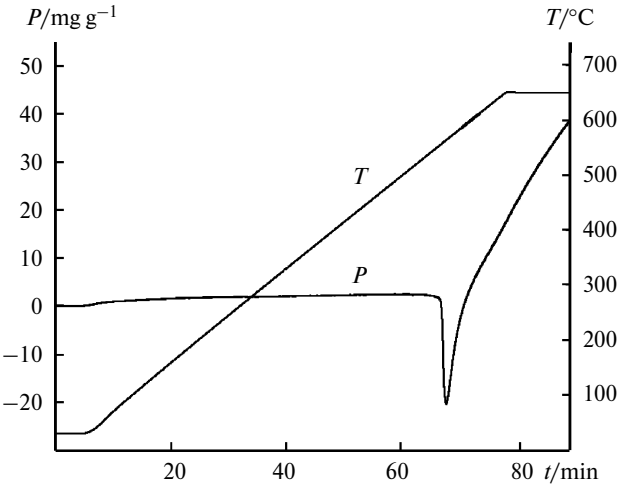

Fig. 9. Thermogravimetric curve for the Ni—Al membrane.

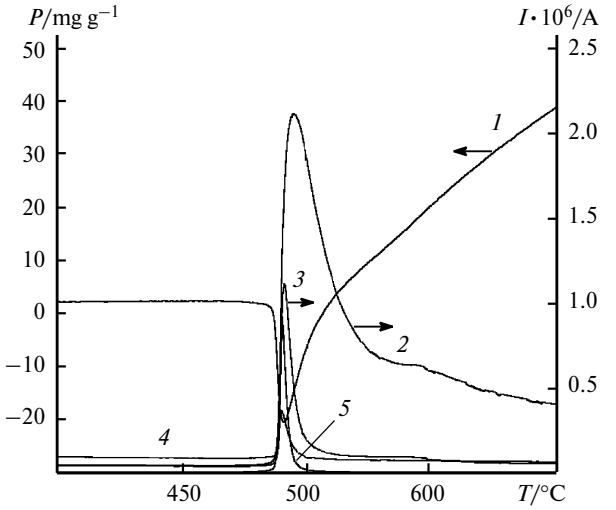

Fig. 10. Thermogravimetric curve for the Ni—Al sample and the results of mass spectrometric analysis of gases formed due to DRM during temperature-programmed heating (10 °C min^{-1}, 30—700 °C; then T = 700 °C): P (*1*), H_2 (*2*), CO (*3*), H_2O (*4*), and CO_2 (*5*).

deposition of carbon on the membrane surface upon methane thermolysis accompanied by hydrogen formation

$$CH_4 \longrightarrow C + 2\,H_2. \qquad (3)$$

When CO_2 was passed successively, a decrease in the sample weight with CO evolution is observed at 520 °C (Fig. 11).

This is related, most likely, to the reaction between CO_2 and carbon formed during thermolysis of methane in reaction (3). The process is accompanied by the evolution of carbon monoxide in the Boudouard retro reaction

$$C + CO_2 \longrightarrow 2\,CO. \qquad (4)$$

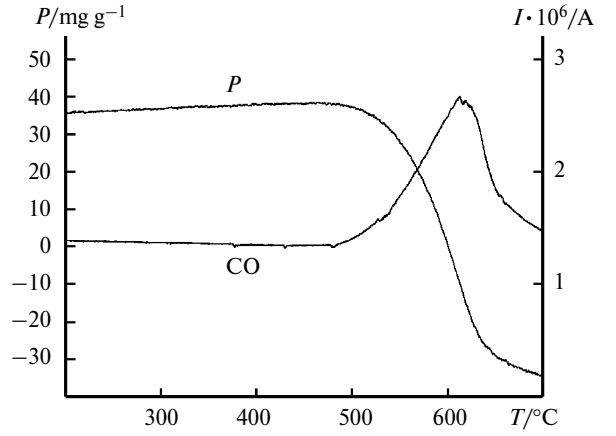

Fig. 11. Thermogravimetric curve for the sample of the initial Ni—Al membrane and the formation of CO as a function of temperature during dry regeneration.

The completion of this reaction on a given sample (see Fig. 11) was observed when the temperature maximum of the experiment was achieved (700 °C).

It has previously[12] been shown that the rate of reaction (4) is an order of magnitude higher than the rate of direct oxidation of methane with air oxygen. These results indicate the high rate of the reaction of carbon dioxide with nanosized carbon formed in microchannels of the membrane, that is, probably, more reactive than bulky carbon.

The data of studies of the membrane material by X-ray diffraction and energy dispersive X-ray analyses confirmed that the initial membrane contained oxide phases of metals.[13]

The gravimetric data characterizing the dynamics of DRM on pelleted MCS **5** and its subsequent dry regeneration in the temperature-programmed regime are presented in Fig. 12.

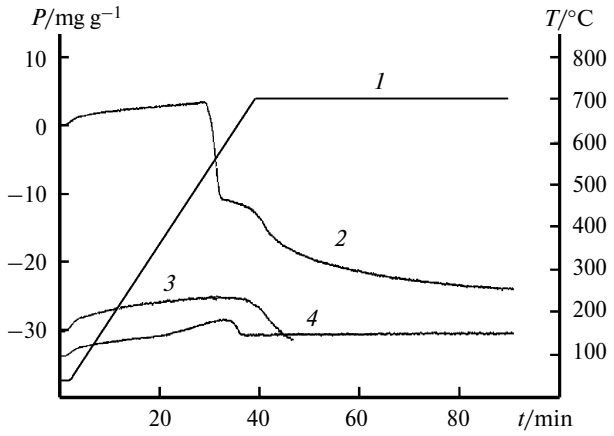

Fig. 12. Dynamics of processes of DRM and dry regeneration on [Pd—Mn]—TiO_2/Ni—Al; *1*, temperature; *2*, DRM; *3*, regeneration of CO_2; *4*, DRM after regeneration.

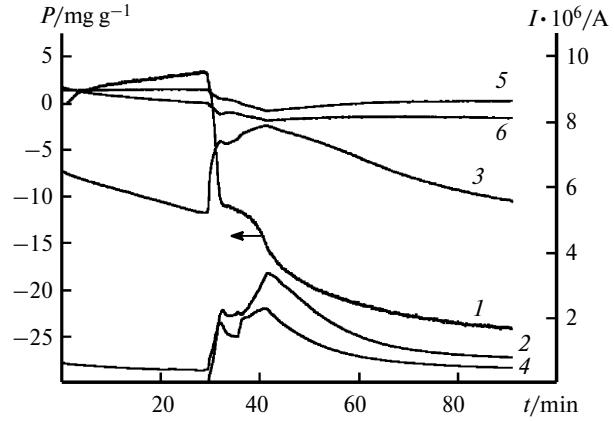

Fig. 13. Thermogravimetric curve for the sample [Pd—Mn]—TiO_2/Ni—Al and the results of mass spectrometric analysis of gases formed by DRM during temperature-programmed heating (10 °C min^{-1}, 30—700 °C; then T = 700 °C): P (*1*), H_2 (*2*), CO (*3*), H_2O (*4*), CO_2 (*5*), and CH_4 (*6*).

As can be seen from Fig. 12, the pattern of the gravimetric curve repeats the shape of the curve found for the initial membrane support. The reaction begins at temperatures ~100 °C lower than that for the initial membrane as indicated by the decrease in the sample weight.

It follows from Fig. 13 that the sample weigh does not increase during DRM, indicating a comparatively small contribution of coking processes occurring on the catalyst sample. The decrease in the sample weight is accompanied by the formation of H_2, CO, and H_2O.

Figure 14 shows that on subsequent heating of the system in a CO_2 flow the MCS is regenerated in the narrow temperature and time intervals.

The dynamics of the DRM dry regeneration processes on the catalytic system [La—Ce]—MgO—TiO_2/Ni—Al (**4**) is analogous to the dynamics of the processes that occur on [Pd—Mn]—TiO_2/Ni—Al (**5**), but the contribution from coking processes is higher on MCS **4**.

The results obtained show that dry reforming of methane proceeds with a high rate in the catalytic channels of the membranes and provides a significant yield of syngas at a short conventional time of contact (~0.1—0.2 s).

The selectivity of the DRM depends on the composition of the catalysts determining different contributions of direct and secondary reactions of the process.

The dynamics of CH_4 and CO_2 transformations observed on the initial membrane and on its membrane catalytic systems indicates that at the first step of the process hydrogen and CO are formed upon the interaction of methane with oxygen of the oxide phases (see reaction (1)). At this step, methane partially undergoes deep oxidation to CO_2 and H_2O in reaction (2). The thermolysis of methane with formation of carbon in reaction (3) is initiated with the temperature increase to 450 °C. Carbon dioxide interacts with carbon to form CO in reaction (4). The rate of this reaction depends strongly on the catalyst composition: in the presence of MCS **5**, the reaction shows a higher rate than the reaction on MCS **4**. It is important that the temperature of the onset of reaction (4) on the MCS is substantially lower than that for the known processes of coal gasification.[14] It is most likely that the intensification of this reaction in the channel of the catalytic membrane is due to high dispersity of carbon formed. The close rates of reactions (3) and (4) in the presence of MCS **5** explain the higher selectivity of this system estimated by the ratio H_2/CO.

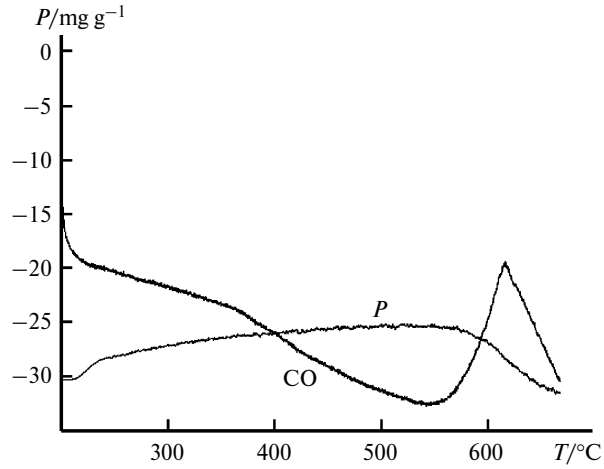

Fig. 14. Thermogravimetric curve for the MCS sample [Pd—Mn]—TiO_2/Ni—Al and the formation of CO as a function of temperature during dry regeneration.

Secondary reactions affecting the selectivity of the process occur along with the direct reactions of DRM. As follows from Fig. 13, the decrease in the rate of water formation at the step of deep methane oxidation (see reaction (2)) indicates that the occurrence of the reversible water—gas shift reaction

$$CO + H_2O \rightleftharpoons CO_2 + H_2, \quad (5)$$

which affects the content of hydrogen in syngas.[15]

It can be assumed that, in the presence of MCS **4**, the backward direction of reaction (5) exerts a stronger effect on the selectivity of the process, due to which the CO content in syngas exceeds the content of H_2.

This work was financially supported by the Russian Foundation for Basic Research (Project Nos 10-03-00715, 09-03-12060-ofi_m, and 08-03-92496-NTsNIL_a).

References

1. M. V. Tsodikov, A. V. Chistyakov, F. A. Yandieva, V. Ya. Kugel, V. I. Uvarov, V. N. Korchak, A. E. Gekhman, I. I. Moiseev, *Tez. dokl. Mezhdunar. nauch. konf. "Europacat IX"* [*Proc. International Scientific Conference "Europacat IX"*] *(Salamanca, Spain, August 30—September 4, 2009)*, Salamanca, 2009, 417.
2. R. Dittmeyer, J. Caro, *Catalytic Membrane Reactors*, in *Handbook of Heterogeneous Catalysis*, Eds G. Ertl, H. Knözinger, F. Schüth, J. Weitkamp, 2nd ed., Wiley-VCH, Weinheim, Vol. **4**, 2008, Ch. 10.7, p. 2198.
3. M. V. Tsodikov, V. V. Teplyakov, M. I. Magsumov, E. I. Shkol´nikov, E. V. Sidorova, V. V. Volkov, F. Kaptein, L. Gora, L. I. Trusov, V. I. Uvarov, *Kinet. Katal.*, 2006, **47**, 29 [*Kinet. Catal.* (*Engl. Transl.*), 2006, **47**].
4. I. M. Kurchatov, N. I. Laguntsov, M. V. Tsodikov, A. S. Fedotov, I. I. Moiseev, *Kinet. Katal.*, 2008, **49**, 129 [*Kinet. Catal.* (*Engl. Transl.*), 2008, **49**].
5. V. I. Uvarov, I. P. Borovinskaya, A. G. Merzhanov, Pat. RF No. 2 175 904, B22F3/10, B22F3/23, C22C1/08—2001; *Byul. Izobret.* [*Invention Bulletin*], 2001, No. 32 (in Russian).
6. M. V. Tsodikov, V. V. Teplyakov, A. S. Fedotov, O. V. Bukhtenko, T. N. Zhdanova, V. I. Uvarov, I. P. Borovinskaya, I. I. Moiseev, Pat. RF No. 2 325 219, B0 1D 71-02, CO 1B 3/38, 2006; *Byul. Izobret.* [*Invention Bulletin*], 2008, No. 15 (in Russian).
7. N. Yu. Kozitsyna, S. E. Nefedov, F. M. Dolgushin, N. V. Cherkashina, M. N. Vargaftik, I. I. Moiseev, *Inorg. Chim. Acta*, 2006, **359**, 2072.

8. G. A. Seisenbaeva, A. V. Shevelkov, J. Tegenfeldt, L. Kloo, D. V. Drobot, V. G. Kessler, *J. Chem. Soc.*, *Dalton Trans.*, 2001, **19**, 2762.
9. A. G. Dedov, A. S. Loktev, I. I. Moiseev, A. Aboukais, J.-F. Lamonier, I. N. Filimonov, *Appl. Catal.*, 2003, **245**, 209.
10. N. Ya. Turova, E. P. Turevskaya, V. G. Kessler, M. I. Yanovskaya, *The Chemistry of Metal Alkoxides*, Kluwer AP, Boston, 2002.
11. A. G. Dedov, A. S. Loktev, K. V. Parkhomenko, M. V. Tsodikov, V. V. Teplyakov, V. I. Uvarov, A. S. Fedotov, I. I. Moiseev, *Khim. Tekhnologiya* [*Chem. Technology*], 2008, 208 (in Russian).
12. M. I. Magsumov, A. S. Fedotov, M. V. Tsodikov, V. V. Teplyakov, O. A. Shkrebko, V. I. Uvarov, L. I. Trusov, I. I. Moiseev, *Ross. Nanotekhnologii* [*Russian Nanotechnologies*], 2006, **1**, 142 (in Russian).
13. A. Fedotov, V. Zhmakin, V. Uvarov, M. Tsodikov, V. Teplyakov, I. Moiseev, *Second German—Russian Seminar on Catalysis — Bridging the Gap between Model and Real Catalysis* (*Kloster Seeon, Bavaria, Germany, March 14—17, 2010*), *Abstrs*, Kloster Seeon, 2010, 24.
14. Yu Zunhong, Gong Xin, Wang Fuchen, *Coal Gasification Technology in China: Application and Development*, Stanford University, Shanghai, 2005; http://gcep.stanford.edu/pdfs/wR5MezrJ2SJ6NfFl5sb5Jg/9_china_wangfuchen.pdf.
15. S. Haag, M. Burgard, B. Ernst, *J. Catal.*, 2007, **252**, 190.

Received November 15, 2010;
in revised form December 22, 2010